Inorganic Chemistry

Article

pubs.acs.org/IC

# Inhibitory Act of Selenoprotein P on $Cu^{+}/Cu^{2+}$-Induced Tau Aggregation and Neurotoxicity

Xiubo Du,[†] Youbiao Zheng,[†] Zhi Wang,[‡] Yijing Chen,[‡] Rui Zhou,[†] Guoli Song,[†] Jiazuan Ni,*[,‡] and Qiong Liu*[,†]

[†]Department of Marine Biology, Shenzhen Key Laboratory of Marine Biotechnology and Ecology and [‡]College of Life Sciences, Shenzhen Key Laboratory of Microbial Genetic Engineering, Shenzhen University, Shenzhen 518060, China

Supporting Information

**ABSTRACT:** Alzheimer's disease (AD) is a neurodegenerative disorder that is characterized by peptide and protein misfolding and aggregation, in part due to the presence of excess metal ions such as copper. Aggregation and cytotoxicity of amyloid-$\beta$ (A$\beta$) peptide with copper ion have been investigated extensively; however, the effects of metalation on tau are less known. Here, we presented the effects of $Cu^{+}$ and $Cu^{2+}$ on aggregation and neurotoxicity of the second repeat unit of the microtubule-binding domain of tau (tau-R2). Tau-R2 was demonstrated to bind 0.44 $Cu^{2+}$ and 0.34 $Cu^{+}$ per monomer with dissociation constants of 1.1 nM and 0.2 pM, respectively. Copper in both oxidation states stimulated the aggregation, ROS production, and neuronal cytotoxicity of tau-R2. We showed that copper-associated tau-R2 aggregates, decreased protein levels of microtubule-associated protein 2 (MAP-2), and synaptophysin in the primarily cultured cortical neurons, reduced mitochondrial density and mobility in the axon and, as a consequence, impaired the growth and probably also the function of neurons. Previously, we reported that the His-rich domain of selenoprotein P (SelP-H) inhibited metal-induced aggregation and toxicity of A$\beta$, due to its metal chelation ability. Here we demonstrated that SelP-H not only inhibited copper-mediated tau aggregation but also interfered with the ongoing aggregation and reversed the already formed aggregates. More intriguing, SelP-H significantly attenuated $Cu^{2+}/Cu^{+}$-tau-R2-induced intracellular ROS production and the impairments of synapse and mitochondrial movement in neurons. This work implies that the surface-exposed His-rich domain of SelP makes it capable of modulating $Cu^{+}/Cu^{2+}$-mediated aggregation and neurotoxicity of both Aß and tau and may play important roles in the prevention of AD progression.

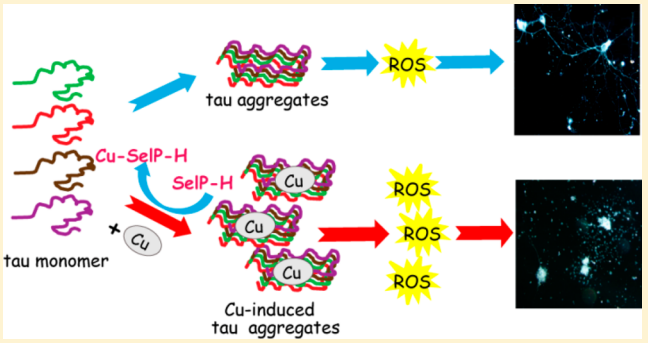


## INTRODUCTION

Alzheimer's disease (AD) is a fatal neurodegenerative disorder that affects one in five people over the age of 85. AD is characterized by two pathological protein deposits, the senile plaques mainly composed of amyloid-$\beta$ (A$\beta$) peptide and the neurofibrillary tangles (NFT) which are bundles of paired helical filaments (PHF) of protein tau. Tau is a highly soluble and natively unfolded protein that binds and promotes the assembly of microtubules. In tauopathies, tau accumulates in the hyperphosphorylated NFT that are visualized within dystrophic neuritis and cell bodies.[1] The amount of tau pathology correlates with progressive neuronal dysfunction, synaptic loss, and functional decline in humans and transgenic mouse models.[2−5] Besides the toxic effect of aggregated tau, a possible loss of its physiological function has been proposed, leading to destabilization of microtubules and impaired axonal transport.

Dyshomeostasis of metal ions such as Cu, Zn, and Fe ions clearly occur in AD brain. These metals bind to the histidine residues of A$\beta$, promote A$\beta$ aggregation and intracellular ROS production, and finally induce neuronal cell death and cognitive deficit. Effects of metals on the aggregation and toxicity of A$\beta$ have been extensively explored.[6] In contrast, very few reports have emerged regarding the role of metals on formation of the hallmark tau deposits of AD. Normally tau protein binds and stabilizes the microtubules in neurons. Hyperphosphorylated tau is observed to aggregate in disease cells.[7] There is accumulating evidence implying that Cu may play an important role in tau's biological function. It is known that the dyshomeostasis of transition metal ions in AD can lead to a local high concentration of copper and that copper ions are involved in the redox reactions occurring in the NFT.[8] The finding that tau protein in the brain contains copper ions has further raised the interest to study the interactions between tau and copper ions.

The interactions between $Cu^{2+}$ and tau or its fragments were reported recently;[9,10] however, the binding property of tau for $Cu^{+}$ is scarce. The reducing environment of the cytosol is expected to stabilize monovalent copper. Information regarding

**Received:** July 28, 2014
**Published:** October 7, 2014

the roles of copper in both oxidation states of $Cu^{+}$ and $Cu^{2+}$ on tau aggregation and neurotoxicity are still lacking. Herein, we present thermodynamic data of tau fragment binding for both $Cu^{+}$ and $Cu^{2+}$. We found copper ions stimulated the aggregation of tau-R2 in vitro and importantly enhanced the toxicity of tau aggregates in living neurons. The effects of Cu ions on tau could be significantly inhibited by a histidine-rich peptide from selenoprotein P (SelP). SelP, an endogenous protein located in the brain with high level, is involved in the response or progression of neurodegenerative disorders, including AD and Parkinson's disease.[11,12] SelP encodes two His-rich regions, located at residues 204−217 and residues 244−250, respectively, which were predicted on the surface of the protein by the PROFace program. Previously, we reported that the His-rich domain of SelP (named SelP-H) blocked metal ions mediated A$\beta$ aggregation, ROS production, and neurotoxicity.[13,14] Here, we extended the study on the function of SelP in modulating the aggregation and toxicity of tau induced by copper ions. Tau fragment R2 (tau-R2) corresponding to the second repeat unit of the microtubule-binding domain lies in the dense core of Alzheimer-PHFs and is pivotal to the biochemical properties of full-length tau protein.[15,16] It was found that the R2 repeat unit exhibited a synergistic effect on the aggregation of tau protein, and R2-included and -deleted tau-isoforms have notable differences in the microtubule-binding ability and PHF-formation tendency.[17] Therefore, we used tau-R2 to mimic the metal binding as well as aggregation properties of tau protein.

## RESULTS AND DISCUSSION

**Thermodynamic Properties of Tau-R2 Binding $Cu^{+}$ and $Cu^{2+}$.** Tau protein, one of the neuronal microtubule-associated proteins (MAPs) in the mammalian brain, has up to 20 isoforms. The microtubule-binding domain (MBD) of tau is located in the C terminus and composed of 3−4 pseudorepeat sequences (named R1, R2, R3, and R4, ~31 residues each). R2 and R3 are essential for aggregation of tau into paired helical filaments (PHFs).[18] The four repeats have a relatively similar and conserved amino acid sequence; however, they are not identical. In particular, R1 and R4 have no Cys, while R3 is the only one possessing two His. Using continuous-wave (CW) ESR, Saxena et al. reported that the equimolar $Cu^{2+}$ complexes of the four repeats are similar to one another in terms of the coordination environment and binding affinity. Pulsed ESR spectra provided direct evidence that a histidine residue and a backbone amide group coordinate to $Cu^{2+}$ in each $Cu^{2+}$−peptide complex. Interestingly, the ESR spectra in terms of both ESR parameters and intensity of a longer peptide containing both R2 and R3 (named tau-R23) with addition of 1, 2, or even 8 equiv of $Cu^{2+}$ ions are quite similar to those of equimolar mixtures of $Cu^{2+}$ and either tau-R2 or tau-R3. Their observations suggest the longer peptide tau-R23 has a $Cu^{2+}$ binding site similar or identical to that of tau-R2 and tau-R3.[9] Consistently, Soragni et al. reported that even a longer tau fragment containing all of the four pseudorepeats coordinates to $Cu^{2+}$ with a stoichiometry value of 1.[19] The two Cys residue containing pseudorepeats tau-R2 and tau-R3 may have a higher possibility to bind the reduced state of $Cu^{+}$ than tau-R1 and tau-R4. In addition, Ma et al. found that $Cu^{2+}$ induced tau-R2 to form more $\alpha$-helix structure than tau-R3, while the $\alpha$-helix structure is responsible for formation of PHFs which aggregate into NFTs.[20,21] Therefore, $Cu^{2+}$ may play a significant role in the aggregation of R2 peptide and tau protein and copper binding to R2 may be another possible involvement in AD. In this study, the second repeat corresponding to the 592−622 region of the canonical isoform PNS-tau was chosen to investigate the effects of copper ions and selenoprotein P on the aggregation and neurotoxicity of tau.

The $Cu^{+}$ binding affinity and stoichiometry value of tau-R2 were determined by competition with bicinchoninic acid (BCA) (details in the Supporting Information). Complexation of $Cu^{+}$ to BCA gives rise to $Cu^{+}(BCA)_2$ with two maximum absorptions at 562 and 358 nm, and the former was used to monitor the competition between a protein and BCA in binding with $Cu^{+}$ (Figure 1A). Addition of tau-R2 led to decreases in the absorption of $Cu^{+}(BCA)_2$, indicating translocation of $Cu^{+}$ from BCA to tau-R2. Absorbance data obtained in tau-R2 titrated into $Cu^{+}(BCA)_2$ (Figure 1, Table S1, Supporting Information) were used to calculate the binding constants for $Cu^{+}$−tau-R2 complex using the Hughes−Klotz equation

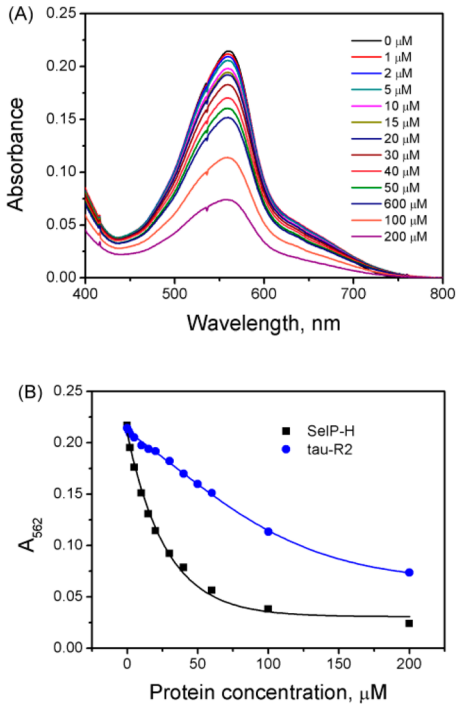


**Figure 1.** Tau-R2 binds $Cu^{+}$. (A) Absorption spectra of 20 $\mu$M $Cu^{+}(BCA)_2$ complex with addition of 0−10 mol equiv of tau-R2. (B) Absorbance at 562 nm with the titration of tau-R2 or SelP-H into 20 $\mu$M $Cu^{+}(BCA)_2$ complex.

$$\frac{1}{Y} = \frac{1}{n} + \frac{1}{nK_a}X$$

where the fractional saturation $Y$ = (concentration of $Cu^{+}$ bound to P)/(total concentration of all forms of P), $X$ = (([BCA]$^2$)/([$Cu^{+}(BCA)_2$])), $K_a$ is the intrinsic binding constant, and $n$ is the stoichiometry value. Detailed information for the calculation of $K_a$ and $n$ can be found in Table S1, Supporting Information.

The slope of the plot of $1/Y$ versus $X$ (Figure S1, Supporting Information) gives log $K_a = 1.9 \times 10^{-5}$ (correlation coefficient $r$ = 0.94, $n$ = 0.34, Figure 1, Figure S1 and Table S1, Supporting Information). Using the known value for the association


dx.doi.org/10.1021/ic501788v | Inorg. Chem. 2014, 53, 11221−11230

constant of $Cu(BCA)_2$ of log $\beta_2$ = 17.30, the binding constant for $Cu^+$ binding to tau-R2 was calculated to be $K_{tau\text{-}R2}$ = 12.58.

As a soft metal, $Cu^+$ prefers to bind soft ligands (Cys-S or Met-S) with triangle or tetrahedral geometries. Therefore, $Cu^+$ might coordinate to the Cys residue in tau-R2 and induce the peptide to form a trimer. Reports describing His−$Cu^+$ interactions are emerging, for example, $Cu^+$ was reported to be ligated by the His13 and His14 in a linear coordination environment in Aß.[26] Previously, we found SelP-H bound $Cu^+$ most probably via its His residues with higher capacity and affinity (log $K_{SelP\text{-}H}$ = 13.44, $n$ = 1.03, correlation coefficient $r$ = 0.99)[14] than tau-R2, making it capable of competing for $Cu^+$ with tau-R2. The abilities of SelP-H and tau-R2 to compete for $Cu^+$ with BCA are compared in Figure 1B.

Generally, His and Cys residues in a peptide are considered to have a higher affinity for $Cu^{2+}$ than the other amino acid. Previously, Saxena et al. demonstrated that tau peptide bound $Cu^{2+}$ via a His residue and a backbone amide group, while the Cys residue was unlikely to be involved in $Cu^{2+}$ coordination.[9] Herein, isotherm titration calorimetry (ITC) was employed to characterize the thermodynamics of tau-R2 binding with $Cu^{2+}$. Representative ITC data for the titration of $Cu^{2+}$ into tau-R2 in *N*-(2-acetamido)-2-aminoethanesulfonic acid (ACES) buffer are shown in Figure 2. The isotherm was best fitted with the

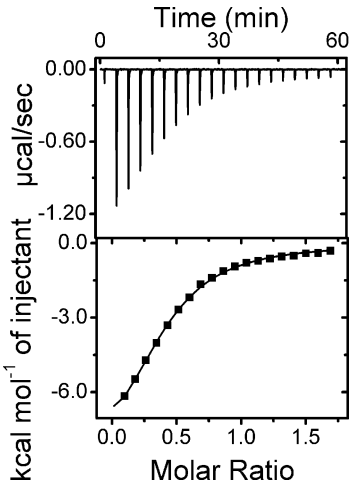


**Figure 2.** Calorimetric titration of $Cu^{2+}$ (2 mM) to tau-R2 (50 $\mu$M) in 20 mM ACES buffer, pH 7.4: (top) raw data; (bottom) plots of integrated heat versus the metal ion/protein ratio. Solid line represents the best fit for single-binding site model. All experiments were carried out at 25 °C.

single-binding-site model with $n$ = 0.44 ± 0.12, and the buffer-dependent parameters are listed in Table 1. Our ITC data suggest that tau-R2 binds $Cu^{2+}$ as a dimer, in line with the previous observation by mass spectrometry.[9] Binding of $Cu^{2+}$ to tau-R2 is an enthalpically driven but entropic penalty process. The buffer-independent binding constant was calculated as described previously.[23−25] The $K_{ITC}$ equation is given as

$$K_{ITC} = \frac{[Cu^{2+} - 2P]}{[Cu^{2+}]_{ITC}([P]_{ITC})^2} \quad (1)$$

where $[P]_{ITC}$ and $[Cu^{2+}]_{ITC}$ represent the fractions of protein and $Cu^{2+}$ that are not found in the metal−protein complex, respectively.

$$[Cu^{2+}]_{ITC} = [Cu^{2+}]_C - [Cu^{2+} - 2P] = [Cu^{2+}] + [ACES - Cu^{2+}] + [2ACES - Cu^{2+}] + [ACES - Cu^{2+} - (H_{-1}ACES)] + [2(H_{-1}ACES) - Cu^{2+}] \quad (2)$$

where $[Cu^{2+}]_C$ represents total $Cu^{2+}$ concentration and $H_{-1}ACES$ represents deprotonated ACES. The pH 7.4 requirement restricts analysis to a single peptide protonation state as represented by eq 3

$$[P]_{ITC} = [P] \quad (3)$$

The expressions for various metal−buffer binding equilibria constants (eqs 4−7) and the buffer-independent $K$ (eq 8) required for analysis are listed below. log $K$ and log $\beta$ values can be found in the reference.

$$K_{MB} = \frac{[ACES - Cu^{2+}]}{[Cu^{2+}][ACES]}; (\log K = 4.32) \quad (4)$$

$$K_{MB2} = \frac{[2ACES - Cu^{2+}]}{[ACES]^2[Cu^{2+}]}; (\log \beta = 7.77) \quad (5)$$

$$K_{M(H_{-1}B)B} = \frac{[2ACES - Cu^{2+}]}{[H][ACES - Cu^{2+} - H_{-1}ACES]}; (\log K = 7.36) \quad (6)$$

$$K_{M(H_{-1}B)_2} = \frac{[2ACES - Cu^{2+}]}{[H][2H_{-1}ACES - Cu^{2+}]}; (\log \beta = 15.34) \quad (7)$$

$$K_{Cu^{2+}-2P} = \frac{[Cu^{2+} - 2P]}{[Cu^{2+}][P]^2} \quad (8)$$

Rearranging eqs 1, 3, and 8 results in eq 9

$$K_{Cu^{2+}-2P} = K_{ITC}\frac{[Cu^{2+}]_{ITC}}{[Cu^{2+}]} \quad (9)$$

Substituting eqs 2 and 4−7 into eq 9 results in eq 10

$$K_{Cu^{2+}-2P} = K_{ITC}\left(1 + K_{MB}[ACES] + K_{MB_2}[ACES]^2 + \frac{K_{MB_2}}{K_{M(H_{-1}B)B}}\frac{[ACES]^2}{[H]} + \frac{K_{MB_2}}{K_{M(H_{-1}B)_2}}\frac{[ACES]^2}{[H]^2}\right) \quad (10)$$

**Table 1. Best-Fit Thermodynamic Parameters of $Cu^{2+}$ Binding to Tau-R2 Obtained from ITC Measurement**

| $n_{ITC}$ | $K_{ITC}$ (×10⁴) | $\Delta H_{ITC}$ [kcal mol⁻¹] | $\Delta S_{ITC}$ [cal mol⁻¹ K⁻¹] | $K$ (×10⁹) | $K_D$ [nM] |
|---|---|---|---|---|---|
| 0.44 ± 0.01 | 6.3 ± 0.3 | −9.5 ± 0.2 | −9.85 | 0.9 ± 0.2 | 1.1 ± 0.2 |


dx.doi.org/10.1021/ic501788v | Inorg. Chem. 2014, 53, 11221−11230

Substituting the value of $K_{ITC}$ into eq 10 provided the buffer-independent binding constant ($K$) and dissociation constant ($K_D$) (Table 1). The buffer-independent dissociation constant of tau-R2 binding for $Cu^{2+}$ was calculated to be 1.1 nM. Previously, the buffer-independent dissociation constant of SelP-H for $Cu^{2+}$ was calculated to be 0.9 nM in identical conditions. The fact that SelP-H binds copper in both oxidation states of $Cu^{+}$ and $Cu^{2+}$ with higher affinities than tau-R2 indicates that SelP-H might modulate $Cu^{+}/Cu^{2+}$-induced aggregation and neurotoxicity of tau-R2.

**Modulation of $Cu^{+}/Cu^{2+}$-Induced Tau-R2 Aggregation by SelP-H.** To study the effects of copper ions on tau aggregation and neurotoxicity, the aggregation kinetics of tau-R2 incubated at 37 °C was examined using a Thioflavin S (ThS) based assay. Heparin was used to initiate the aggregation of tau-R2. A fast increase in ThS fluorescence was observed in accordance with a typical two-phase growth curve (Figure 3). The kinetic curves of fibrillization were fitted well to the sigmoidal function Boltzmann equations. Both $Cu^{+}$ and $Cu^{2+}$ promoted the aggregation of tau-R2, reflected by higher ThS fluorescence intensity. SelP-H almost completely surpressed the roles of Cu ions, presenting similar aggregation profiles as that of tau-R2 incubated in the absence of $Cu^{+}/Cu^{2+}$.

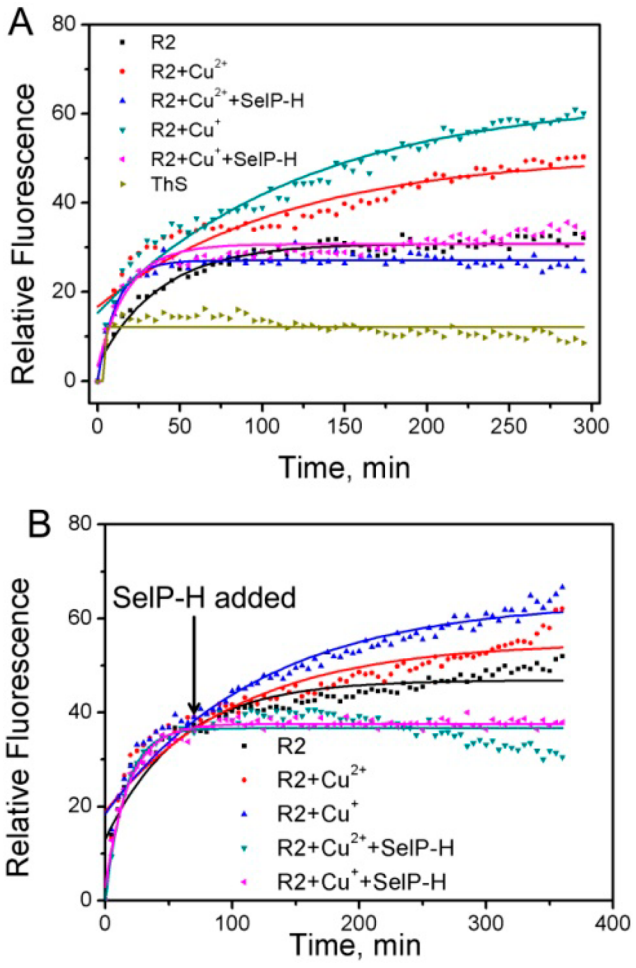


**Figure 3.** Fibrillation of tau-R2 in different conditions. Tau-R2 (15 $\mu$M) was incubated with heparin (3.8 $\mu$M) with or without $Cu^{2+}/Cu^{+}$ (7 $\mu$M). SelP-H (10 $\mu$M) was added at the beginning of the incubation (A) or 1 h later (B). All experiments were carried out in 50 mM Tris-HCl, 100 mM NaCl, containing 20 $\mu$M ThS at pH 7.4, 37 °C. $\lambda_{ex}$ = 440 nm, $\lambda_{em}$ = 480 nm. Solid lines represent fits of the data to the Boltzmann equation.

The aggregation morphology and the extent of tau-R2 aggregation were further investigated by transmission electron microscopy (TEM). The freshly prepared tau-R2 solution showed fibrillogenesis after incubation with heparin at 37 °C for 6 h (Figure 4a). Cu ions in both oxidation states of $Cu^{+}$ and $Cu^{2+}$ promoted the fibrillization of tau-R2 with good agreement with ThS fluorescence assay. In the presence of $Cu^{2+}$, tau-R2 aggregated intensively to form abundant ribbons and twisted chains of a complex of protofibrils and fibrils (Figure 4b). The fibrils were much longer and bolder. $Cu^{+}$ stimulated the fibrils to be tangled up, and a network-like morphology was formed (Figure 4e). SelP-H shows a strong inhibitory effect on the $Cu^{+}/Cu^{2+}$-induced tau-R2 aggregation, with little aggregates observed in the TEM images (Figure 4c and 4f).

Interestingly, when the already formed metal−tau-R2 aggregates were incubated with SelP-H for another 24 h, the aggregates were disassembled, suggesting a disaggregate effect of SelP-H (Figure 4d and 4g). This effect was further confirmed by Thioflavin T (ThT) fluorescence assay.

The fibril contents of tau samples a−g in Figure 4 were compared by ThT fluorescence intensity at 482 nm. ThT can specifically bind to the $\beta$-sheet structure rapidly but not to monomer or oligomer intermediates. Therefore, the fluorescence intensity at 482 nm is in line with the quantity of fibrils. As clearly shown in Figure 5A and 5B, the extent of tau aggregation decreased dramatically after incubation with SelP-H for 24 h, as reflected by a very weak ThT fluorescence intensity.

We also examined whether SelP-H was able to interfere with the ongoing aggregation of tau-R2 induced by Cu ions by incubating tau-R2 and Cu ions for 1 h before 10 $\mu$M SelP-H was added to the mixture. The aggregation kinetics and intensity were measured by ThS- and ThT-based fluorescence assay, respectively (Figures 3B and 5). As shown in Figure 3B, the aggregation of tau-R2 induced by Cu ions was stopped almost immediately when SelP-H was added to the mixture. Consistently, the ThT fluorescence intensity at 482 nm of this sample is quite close to that of tau-R2 aggregated alone (Figure 5). These observations implied that SelP-H not only inhibited metal-induced tau aggregation but also interfered with the ongoing aggregation and disaggregated the already formed aggregates.

**SelP-H Attenuates ROS Production and Neurotoxicity Induced by $Cu^{2+}/Cu^{+}$-tau-R2 Aggregates.** $Cu^{2+}$ binding to Aß promoted its aggregation, neurotoxicity, as well as intracellular ROS production. In this work, we measured the viabilities along with the ROS concentrations of mouse neuroblastoma cells N2A upon treatment with tau-R2 aggregates prepared in different conditions for 24 h. Cell viability was determined by CCK-8 assay, while ROS levels were detected with the fluorescent probe DCFH and quantified with flow cytometry. Tau-R2 aggregates were prepared similarly as in the TEM study. Figure 6A shows that when N2A cells were incubated with tau-R2 fibrillar aggregates, a decrease in the viability of N2A cells (86.6 ± 3.5% cell viability) was observed as compared with the control group. Meanwhile, tau-R2 fibrils promoted the ROS production in N2A cells by 1.65 ± 0.13 fold (Figure 6B). To our knowledge, this is the first report that tau fibrillar aggregates induce generation of ROS, as Aß fibrils does. SelP-H reduced both the ROS production and the toxicity caused by tau-R2 fibrils. Neither $Cu^{+}$ nor $Cu^{2+}$ at a


dx.doi.org/10.1021/ic501788v | Inorg. Chem. 2014, 53, 11221−11230

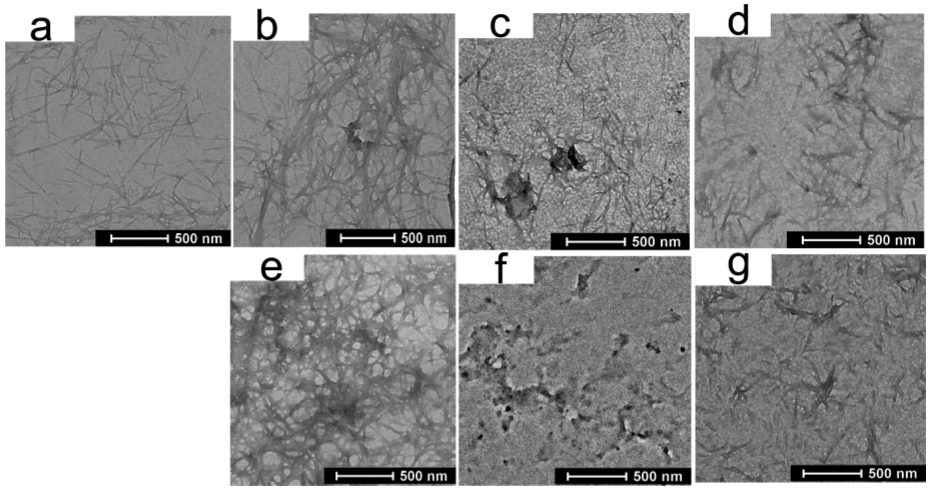


**Figure 4.** Transmission electron microscopy images of tau-R2 (a), tau-R2 with $Cu^{2+}$ (b), tau-R2 with $Cu^{2+}$ and SelP-H (c), tau-R2 with $Cu^{+}$ (e), tau-R2 with $Cu^{+}$ and SelP-H (f), after incubation at 37 °C for 6 h. (d and g) Formed $Cu^{2+}$ and $Cu^{+}$-associated tau-R2 aggregates were incubated with SelP-H for 24 h before TEM imaging. Final concentrations of tau-R2, $Cu^{2+}/Cu^{+}$, and SelP-H are 15, 7, and 10 $\mu$M, respectively. $Cu^{+}$ was prepared by reducing $CuSO_4$ with 1 mM ascorbic acid. Scale bar = 500 nm.

concentration of 7 $\mu$M significantly stimulated ROS generation in N2A cells. However, $Cu^{+}/Cu^{2+}$-associated tau-R2 complexes increased ROS levels by 2.04 ± 0.17 and 1.69 ± 0.01 fold relative to tau-R2 aggregates, respectively (Figure 6B). Accordingly, $Cu^{2+}$ and $Cu^{+}$ substantially enhanced the toxicity of tau-R2, attenuating the cell viability to 36.8 ± 5.3% and 26.7 ± 3.7%, respectively (Figure 6A). In contrast, the aggregates of tau-R2 coincubated with both $Cu^{2+}/Cu^{+}$, and SelP-H demonstrated much lower neurotoxicity, with survival rates increased to 56.1 ± 1.5% and 69.6 ± 8.6%, respectively. SelP-H significantly decreased ROS production caused by $Cu^{+}/Cu^{2+}$–tau-R2 complexes, almost to the control level. The results revealed that SelP-H showed good protection against the tau-R2 neurotoxicity promoted by Cu ions, especially in the case of $Cu^{+}$. Previously, we found the neurotoxicity of $A\beta_{42}$ induced by $Cu^{+}$ and $Cu^{2+}$ could be significantly restored by SelP-H. Consequently, the high $Cu^{+}/Cu^{2+}$ binding affinity of SelP-H makes it capable of modulating the aggregation and neurotoxicity of the two AD-related peptides induced by Cu ions. The significant correlation between the ROS production induced by various tau aggregates and their neurotoxicity suggested that ROS might be a critical factor responsible for cytotoxicity induced by tau aggregates, which is similar to the case of Aß.

Aggregation of intact tau protein in vitro was demonstrated to be dependent on the presence of heparin,[27] which was also found in the Alzheimer-NFT in vivo. However, in our study, the aggregation profile of tau-R2 was observed to be quite similar in the presence or absence of heparin by TEM imaging and ThS fluorescence assay (data not shown). We propose that the second repeat unit of tau is more prone to aggregate than the intact protein. The cell viability and ROS assay revealed that tau-R2 aggregates prepared with heparin are slightly more toxic than aggregates without heparin, which could be resorted by SelP-H (Figure 6). ThS fluorescence showed that SelP-H decreased the aggregation of tau-R2 only by a little extent in the absence of copper ions (Figure S2, Supporting Information).The His-rich domain of rat SelP was previously reported to bind heparin under some conditions.[28] The isotherm profiles of SelP-H titrated with heparin at pH 6.5–7.4 suggested a very weak, if any, interaction between them. In addition, the direct interaction between SelP-H and tau-R2 was not supported by ITC study (data not shown). Therefore, the inhibitory effect of SelP-H on the aggregation and toxicity of $Cu^{+}/Cu^{2+}$–tau complex should be most attributed to its ability to compete for $Cu^{+}/Cu^{2+}$, although SelP-H might also mildly interfere with the interaction between tau-R2 and heparin.

**SelP-H Protects Primary Neurons Against $Cu^{2+}/Cu^{+}$-tau-R2 Aggregates.** Dark field microscopy (DFM) was used to directly view the growth status of primary neurons upon treatment of different tau-R2 aggregates for 12 h. As shown in Figure 7B, neurons incubated with tau-R2 aggregates prepared in the absence of Cu ions were grown almost as well as those cultured in normal media, with a long axon and abundant dendrites. Furthermore, connections between neurons were observed to support normal synaptic functions. When incubated with tau-R2 aggregates prepared in the presence of $Cu^{2+}$, a large amount of neurons were killed. The survived neurons showed a very short axon and little dendrite branching. The situation of neurons cultured with $Cu^{+}$–tau-R2 aggregates was even worse. The neurons were degraded, and almost no neurite was observed. In both cases, communication between neurons was absolutely disrupted. SelP-H showed a noticeable protection effect for primary neurons against Cu–tau-R2 aggregates. Neurons were grown as healthily as the control group.

Microtubule-associated protein 2 (MAP-2) is a neuron-specific marker. This protein is a cytoskeleton member that is detected mainly in dendrites. MAP-2 affects the shape, polarity, and plasticity of neurons by controlling microtubule assembly. Disturbed expression of MAP-2 is suggested to induce impairments in the stability of dendrites and synaptic signal transduction. Immunostaining against MAP-2 of neurons after cultured in different tau-R2 aggregates was performed. We found the immunoreactivity of MAP-2 in neurons was significantly decreased upon treatment of Cu–tau-R2 aggregates, relative to the control group as well as neurons treated with either tau-R2 aggregates or SelP-H-Cu-tau-R2 aggregates (Figure 8). Synaptophysin, a synaptic vesicle protein whose distribution and abundance provides a synaptic marker in neurons, was also immunostained, as shown in Figure 9. We found synaptophysin was significantly decreased in Cu–tau-R2-


dx.doi.org/10.1021/ic501788v | Inorg. Chem. 2014, 53, 11221–11230

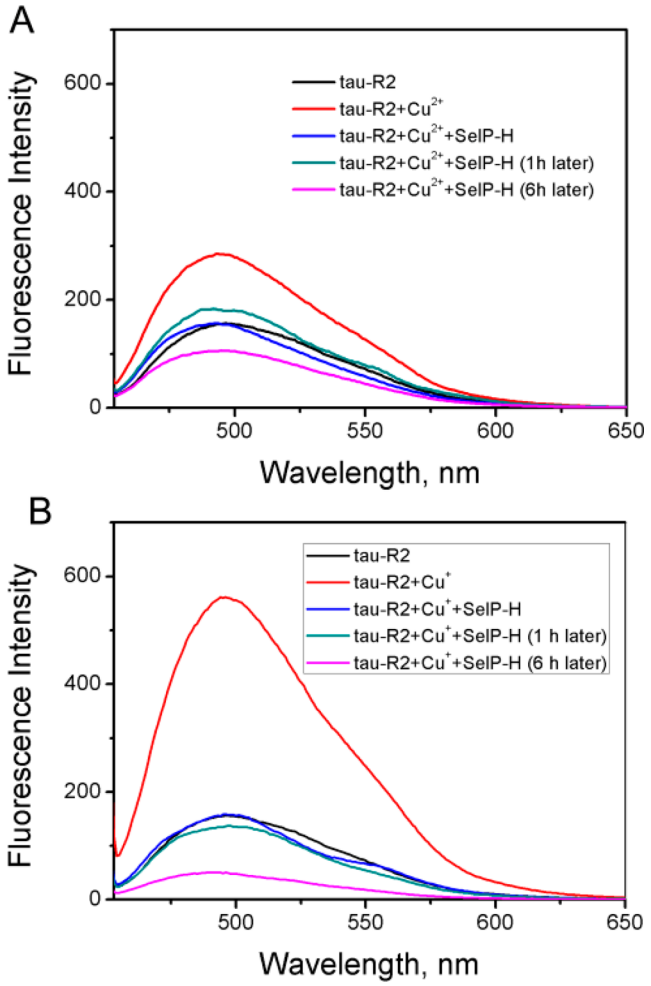


**Figure 5.** Fibrils contents of tau-R2 aggregates prepared in different conditions. Tau-R2 (15 $\mu$M) was incubated with heparin in the presence or absence of $Cu^{2+}/Cu^{+}$ (7 $\mu$M) at 37 °C for 6 h, before ThT fluorescence was recorded. SelP-H (10 $\mu$M) was added either at the beginning of incubation, 1 h after incubation, or 6 h later and further incubated for another 24 h. All experiments were carried out in 50 mM Tris-HCl, 100 mM NaCl, containing 20 $\mu$M ThT at pH 7.4, 37 °C. $\lambda_{ex}$ = 444 nm.

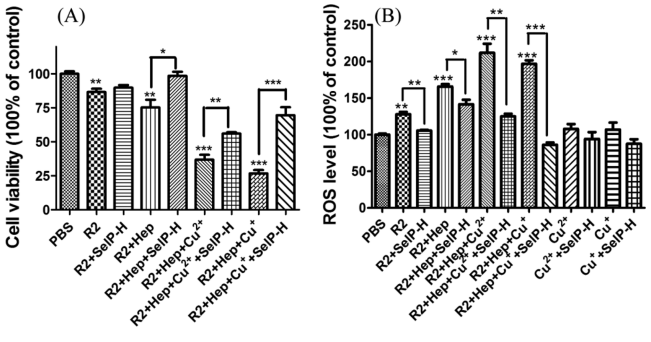


**Figure 6.** Toxic effects of different tau-R2 aggregates to N2A cells. (A) CCK-8 cell viability assay of N2A cells upon treatment with tau-R2 aggregates prepared in indicated conditions. (B) ROS levels in N2A cells upon treatment with different tau-R2 aggregates. Final concentrations of SelP-H, tau-R2, and Cu ions are 10, 15, and 7 $\mu$M, respectively. $Cu^{+}$ was prepared by reducing $CuSO_4$ with 1 mM ascorbic acid. Results were obtained from the average of three experiments: (*) $P < 0.05$; (**) $P < 0.01$; (***) $P < 0.001$.

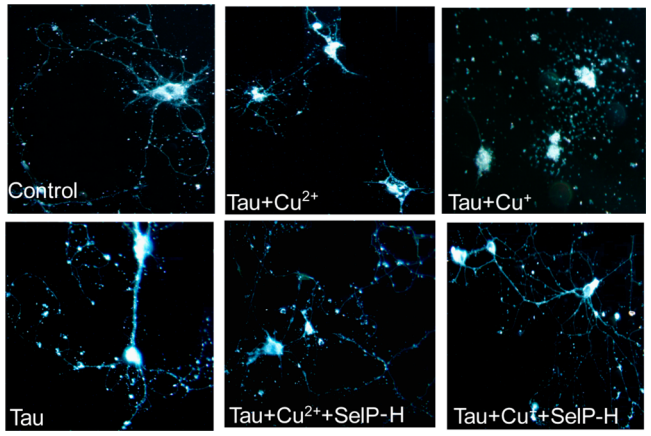


**Figure 7.** Typical dark field microscopy (DFM) images of primary neurons upon 12 h treatment with tau-R2 aggregates prepared in indicated conditions. Final concentrations of SelP-H, tau-R2, and Cu ions are 5, 7.5, and 3.5 $\mu$M, respectively. $Cu^{+}$ was prepared by reducing $CuSO_4$ with 1 mM ascorbic acid.

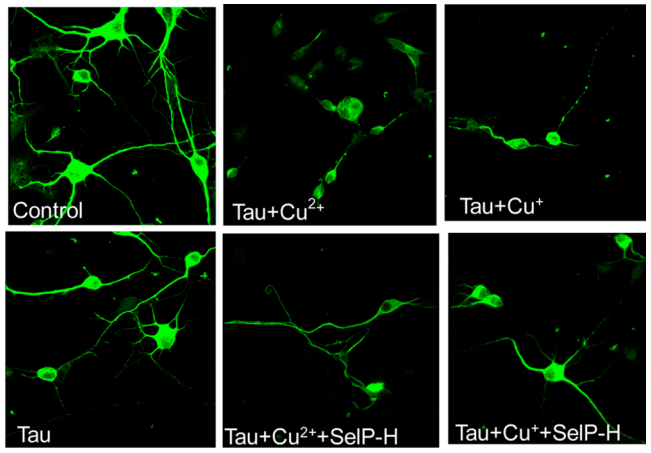


**Figure 8.** Typical confocal images showing the level and distribution of MAP-2 in primary neurons upon 12 h treatment with tau-R2 aggregates prepared in indicated conditions. Final concentrations of SelP-H, tau-R2, and Cu ions are 5, 7.5, and 3.5 $\mu$M, respectively. $Cu^{+}$ was prepared by reducing $CuSO_4$ with 1 mM ascorbic acid.

treated neurons, indicating that Cu−tau-R2 aggregates affect synaptic growth. With addition of SelP-H, the immunoreactivity of synaptophysin was comparable with the control group. These observations further confirm the protective effect of SelP-H against Cu-tau-R2 toxicity.

In our study, copper ions were incubated with tau-R2 and SelP-H for 12 h before being added to the neurons. The concentration of free copper in the mixture was very low, considering the very high affinity of tau-R2 and SelP-H for both $Cu^{+}$ and $Cu^{2+}$. However, we still investigated the effects of $Cu^{+}$ and $Cu^{2+}$ on neuronal growth. The dark field images showed that both $Cu^{+}$ and $Cu^{2+}$ at concentrations of 3.5 $\mu$M impaired growth of neurons, which could be prevented with addition of SelP-H (5 $\mu$M) (Figure S3, Supporting Information). Upon treatment of $Cu^{+}$ or $Cu^{2+}$ for 12 h, the expression levels of both MAP2 (Figure S4, Supporting Information) and synaptophysin (Figure S5, Supporting Information) were decreased. In the presence of SelP-H, the toxic effects of $Cu^{+}$ and $Cu^{2+}$ were surpressed. Therefore, SelP-H is dual functional, protecting


dx.doi.org/10.1021/ic501788v | Inorg. Chem. 2014, 53, 11221−11230

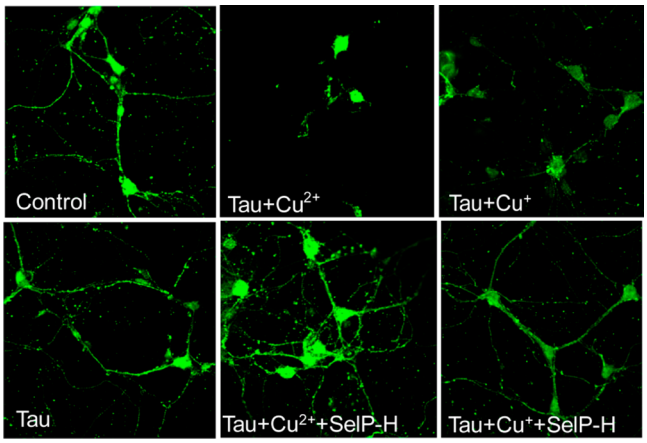


**Figure 9.** Typical confocal images showing the level and distribution of synaptophysin in primary neurons upon 12 h treatment with tau-R2 aggregates prepared in indicated conditions. Final concentrations of SelP-H, tau-R2, and Cu ions are 5, 7.5, and 3.5 $\mu$M, respectively. $Cu^{+}$ was prepared by reducing $CuSO_4$ with 1 mM ascorbic acid.

neurons from the toxicities of both copper ions and copper ions-mediated tau-R2 aggregates.

**Axonal Mitochondrial Mobility of Neurons Exposed to Different Tau-R2 Aggregates.** To fulfill their synaptic roles, such as energy supply maintenance, calcium buffering, synaptic transmission, and vesicle release, mitochondria must transport from the soma to distal synapses via mitochondrial transport and constantly reconfigure to meet synaptic needs. Previously, people found Aß aggregates reduced mitochondria mobility in axons significantly.[29,30] Here, we monitored mitochondrial trafficking within axonal processes of neurons upon treatment of different tau-R2 aggregates for 12 h. In tau-R2-treated cultures, we observed significantly decreased mitochondrial density and mobility, relative to the PBS vehicle-treated neurons. Axonal mitochondria were almost stationary when the neurons were exposed to tau-R2 aggregates with $Cu^{+}$ or $Cu^{2+}$. As expected, SelP-H attenuate the toxic effects of $Cu^{+}$ or $Cu^{2+}$−tau aggregates toward axonal mitochondria, with several mobile mitochondria observed in the SelP-H−$Cu^{+}$/$Cu^{2+}$−tau-R2-superimposed neurons (Figure 10).

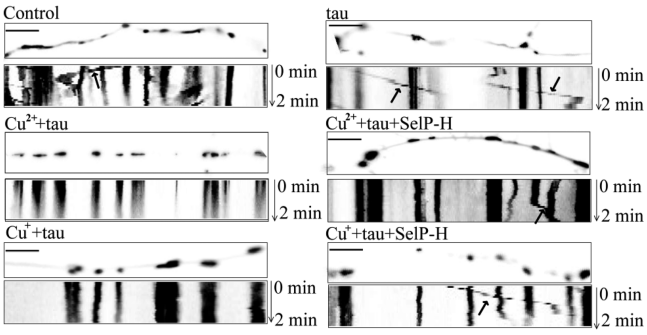


**Figure 10.** Representative kymograph images of axonal mitochondrial movement upon 12 h treatment with tau-R2 aggregates prepared in indicated conditions. (Top and bottom) Distribution and movement of mitochondria in the axons, respectively. Final concentrations of SelP-H, tau-R2, and Cu ions are 5, 7.5, and 3.5 $\mu$M, respectively. $Cu^{+}$ was prepared by reducing $CuSO_4$ with 1 mM ascorbic acid (scale bar = 10 $\mu$m).

Synapses are ultrastructural sites for memory storage in the brain, and synaptic damage is the best pathologic correlate of cognitive decline in AD. An important aspect of synaptic plasticity in the brain is axonal transport of essential components such as mitochondria from the soma to the synapse. Several reports have shown that overexpression of human tau[40] in neurons decreased axonal mitochondrial trafficking.[31−33] In our study, we found extracellular tau aggregates, especially in the presence of $Cu^{+}$ or $Cu^{2+}$, also impair the transport of axonal mitochondrial. Copper is an essential micronutrient that plays a central role for a broad range of biological processes. We demonstrated that both $Cu^{+}$ and $Cu^{2+}$ promoted the aggregation of tau-R2, which could be inhibited by SelP-H. Tau-R2 aggregates, especially in the presence of $Cu^{+}$ or $Cu^{2+}$, decreased protein levels of MAP-2 and synaptophysin, the specific markers of neuron and synapse, reduced mitochondrial density and mobility in the axon and killed neurons. Tau is a microtubule-associated protein that forms intracellular aggregates in several neurodegenerative diseases collectively termed tauopathies, including Alzheimer's disease. One model for the pathogenesis of the tauopathies holds that aggregates produced in one cell escape or are released into the extracellular space to promote aggregation in neighboring or connected cells.[34−38] Release of tau by neurons had previously been documented, although the mechanism of release is still a matter of debate.[39−41] There is compelling evidence that the intracellular milieu does not contain any free copper ions;[42] consequently, the likelihood of interaction between tau and Cu ions inside the cell is a contentious issue. However, people did detect Cu ions in tau in the brain. One possibility is that the rapid kinetics of copper uptake and release might provide a labile intracellular copper pool.[43] However, it is more possible that the extracellular copper binds the released tau and promotes its aggregation, which is then reuptaked by adjacent cells and trigger fibril formation of native tau inside cells. Studies suggested increased levels of exogenous tau may cause a greater pathological risk to patients than hitherto suspected. Here we demonstrated the neurotoxicity of tau aggregates with copper undoubtedly, either by promoting ROS generation or by triggering the spread of tau pathology.

Among the 25 human selenoproteins, SelP is widely expressed in the brain and involved in the onset and progression of AD; however, the underlying mechanisms of which are far away from clear. SelP was found to be colocated with Aß plaques and NFT in AD brains.[44] In SelP, there are three domains (N-terminal region, C-terminal region, and His-rich domain, SelP-H) predicated on the surface of the protein. The functions of the N-terminus and C-terminus were previously reported to encompass oxidant defense and Se homeostasis.[45,46] However, the His-rich domain was less studied. In previous work, we found SelP-H bound transition metal ions and surpressed metal-mediated $Aß_{42}$ aggregation, ROS generation, and toxicity.[13,14] Here we extended the roles of SelP-H to regulate both $Cu^{+}$- and $Cu^{2+}$-mediated aggregation and neurotoxicity of the tau fragment. As mentioned above, the inhibitory effect of SelP-H on the aggregation and neurotoxicity of $Cu^{+}$/$Cu^{2+}$−tau complex was most attributed to its ability to compete for $Cu^{+}$/$Cu^{2+}$. Therefore, we suggest a chelator with higher $Cu^{+}$/$Cu^{2+}$ affinities than tau may have a similar effect as SelP-H. However, it should be noted that SelP-H has moderate $Cu^{+}$ and $Cu^{2+}$ binding affinities ($K_D$ = 3.7 × $10^{-14}$ and 0.9 nM, respectively),[14] i.e., higher than those of $Aß_{42}$ and tau-R2 while much lower than those of Cu-dependent enzymes such as SOD


dx.doi.org/10.1021/ic501788v | Inorg. Chem. 2014, 53, 11221−11230

($K_D$ = 6 fM).[42] Consequently, SelP-H may inhibit the interaction between copper and $A\beta_{42}$ or tau, but not extract copper ions from metalloenzymes that need this cation as an essential element of their active sites. Our study implies that the surface-exposed His-rich domain of SelP makes it capable of modulating $Cu^+/Cu^{2+}$-mediated aggregation and toxicity of both Aß and tau and may play important roles in prevention of AD progression.

## EXPERIMENTAL SECTION

**Determination of $Cu^+$-tau-R2 Dissociation Constant.** Tau-R2 (corresponding to the 592−622 region of PNS-tau: VQIIN KKLDL SNVQS KCGSK DNIKH VPGGGS) was synthesized at ChinaPeptides Co., Ltd. Bicinchoninic acid is a colorimetric $Cu^+$ chelator, which can form a stable purple complex with $Cu^+$ in a 2:1 ratio as $Cu^+(BCA)_2$ that exhibits absorption maxima at 562 ($\varepsilon$ = 7900 $M^{-1}\cdot cm^{-1}$) and 358 nm ($\varepsilon$ = 42 900 $M^{-1}\cdot cm^{-1}$).[22] Therefore, transfer of $Cu^+$ from BCA to the protein can be monitored by the decrease in UV−vis absorbance of $Cu^+(BCA)_2$ at 562 or 358 nm.

Studies of the competition reaction between BCA and tau-R2 were carried out under anaerobic conditions as described previously.[27,28] Briefly, $Cu^+$ in the form of $[Cu(MeCN)_4]PF_6$ was mixed with BCA in a molar ratio of 1:3 in Tris/HCl buffer (50 mM, pH 7.4) as a stock solution. Tau-R2 solution at various concentrations was then mixed with the stock solution to give rise to a final concentration of $Cu^+$ of 20 $\mu$M and BCA of 60 $\mu$M. Ascorbic acid was kept at 1 mM to maintain the oxidation state of $Cu^+$ in the reaction mixture. To ensure the equilibrium was reached, the mixture was incubated at room temperature for at least 1 h (no additional change in absorption was observed). Results were corrected for dilution and baseline absorbance at 800 nm.

**Isothermal Titration Calorimetry (ITC).** ITC measurements were carried out at 25 °C on a MicroCal iTC-200 microcalorimeter (Northampton, MA). Tau-R2 was prepared in 20 mM ACES buffer at pH 7.4, with the ionic strength adjusted to 100 mM with NaCl. The titrant was made by mixing appropriate amounts of a stock solution of $CuSO_4$ (10 mM in nanopure Milli-Q water) with ACES buffer. The metal concentration of the stock solution was determined by ICP-MS.

Briefly, 2 $\mu$L of 2 mM $CuSO_4$ was titrated into 200 $\mu$L of 50 $\mu$M protein over 4 s with a 3 min interval between each injection. Twenty injections were made in total. The reaction solution was stirred at 1000 rpm. The heat of dilution, mechanical effects, and nonspecific interactions were accounted for by averaging the last three points of titration, and the value was subtracted from all data points. Results were analyzed by Origin 7.0 (Microcal) using a one-site binding model. A nonlinear least-square method was used to obtain the best-fit parameters for the number of binding sites, $n$, the association constant, $K_a$, and the changes of enthalpy, $\Delta H$, and entropy, $\Delta S$ (Table S2, Supporting Information). All of the experiments were performed in triplicate under the same conditions.

**Thioflavin S (ThS) and Thioflavin T (ThT) Fluorescence.** Fibrillization of tau-R2 in different conditions was monitored by ThS fluorescence. Freshly prepared tau-R2 was mixed with heparin and $Cu^{2+}/Cu^+$; SelP-H was added into the mixture immediately or 1 h later. SelP-H was overexpressed and purified as described previously.[13] Samples in 200 $\mu$L were added to 96-well plates and incubated at 37 °C. The ThS fluorescence intensity of each sample was recorded using a microplate reader (Fluoroskan Ascent FL, Thermo Scientific) with 440/480 nm excitation/emission filters at different time points. The assay was performed in triplicate and repeated at least twice. The fibrils contents of tau-R2 incubated with or without $Cu^{2+}/Cu^+$ and SelP-H at 37 °C for 6 h were measured by ThT fluorescence. Fluorescence spectra of each sample were recorded using a fluorescence spectrophotometer (Fluoroskan Ascent FL 4500, Thermo Scientific) with 444 nm as the excitation filter. The final concentrations of tau-R2, heparin, $Cu^{2+}/Cu^+$, and SelP-H are 15, 3.8, 7, and 10 $\mu$M, respectively.

**Transmission Electron Microscopy (TEM).** Tau-R2 (15 $\mu$M) was incubated with heparin (3.8 $\mu$M) in the presence or absence of $Cu^{2+}/Cu^+$ (7 $\mu$M) and SelP-H (10 $\mu$M) at 37 °C for 6 h. Then each sample (5 $\mu$L) was put on glow-discharge, Formvar/carbon 300 mesh copper grids (Pacific Grid-Tech) and incubated at room temperature for 2 min. Excess solution was removed with filter paper, and the grids were rinsed twice with $H_2O$. Then the grids were stained with uranyl acetate (1% w/v, $H_2O$, 5 $\mu$L) for 1 min, blotted with filter paper, and dried for 15 min at room temperature. Samples were visualized with a transmission electron microscope (FEI Tecnai G2 TEM) at 200 kV and ×29 000 magnification.

**Cell Culture.** N2A cells were maintained in Dulbecco's modified Eagle's Medium (DMEM) supplemented with 10% FBS, 100 U/mL penicillin G, and 100 $\mu$g/mL streptomycin, and cultured at 37 °C, 5% $CO_2$ incubator. Cells in the logarithmic phase were digested with trypsin and seeded in 96-well or 6-well plates, resulting in about 0.5 × $10^3$ cells in 100 $\mu$L medium or $10^5$ cells in 2 mL medium per well, for CCK-8 assay or ROS measurement, respectively. Cells were incubated at 37 °C, 5% $CO_2$ for 24 h to attach the plates. The tau-R2 stock solution was diluted to a final concentration of 15 $\mu$M in FBS-free DMEM containg 3.8 $\mu$M heparin and 7 $\mu$M $Cu^{2+}/Cu^+$ and incubated at 37 °C for 1 h; then an appropriate amount of SelP-H (with a final concentration of 10 $\mu$M) in DMEM was added to the solution, and the mixture was incubated at 37 °C for 6 h before being added to the cells. For CCK-8 or ROS assay, 50 $\mu$L or 2 mL of each preincubated tau-R2 sample (with or without addition of $Cu^{2+}/Cu^+$ and SelP-H) was diluted with fresh FBS-free DMEM medium and added individually to the cell well. The same volume of serum-free medium was added into control cultures (only N2A cells present). Cells were then incubated for an additional 24 h at 37 °C. At the end of incubation, cell viability was determined by the CCK-8 assay and ROS level was determined by the DCF method.

**Cell Viability Assay.** Twenty microliters of CCK-8 reagent (Beyotime, Shanghai CHN) was added to each well, and the cells were incubated at 37 °C for further 2 h. The absorbance at 450 nm was measured with a reference wavelength at 650 nm using a SpecTRA MAX 190 microplate reader (Molecular Devices, Sunnyvale, CA, USA). Triplicates were performed throughout the procedures.

**Measurement of ROS.** Before measurement, the old medium was removed from the cells and 2 mL of 2′,7′-dichlorofluorescin diacetate (DCFH-DA, 10 $\mu$M in FBS-free medium) was added into each well. Cells were incubated at 37 °C for further 20 min and washed three times with FBS-free medium. Cells were harvested and washed three times with ice-cold PBS and resuspended in PBS. The intensity of fluorescence was analyzed by flow cytometry (FACS Calibur, Becton Dickinson) with excitation at 488 nm and emission at 535 nm. A gate was set to exclude signals from debris and aggregates. Results are expressed as fold change.

**Neuronal Culture.** Primary cultured cortical neurons were obtained from day 1 pups of B6129SF2/J mice. Briefly, cerebral cortices were dissected from the brain and digested with 0.4 mg/mL papain at 37 °C for 30 min. Digested tissue was triturated with pipetting in DMEM with 10% FBS. Dissociated cells were cultured in the neurobasal medium with 2% B27 supplement, 0.5 mL of L-glutamine (Invitrogen), and 50 U/mL of penicillin-streptomycin using poly-D-lysin (Sigma-Aldrich) and seeded in glass coverslips precoated with poly-D-lysine and incubated in 24-well cell culture plates. The medium was completely replaced after 4 h, and then one-half of the medium was replaced every 3 days. At day 7, the cultured neurons were treated with tau aggregates (7.5 $\mu$M tau-R2, 3.5 $\mu$M $Cu^+/Cu^{2+}$, 5 $\mu$M SelP-H, and 1.9 $\mu$M heparin, incubated at 37 °C for 6 h before added to the neurons) for 12 h before imaging through dark field microscope and confocal microscope.

**Dark Field Microscopy.** Dark field microscopy (DFM) was performed on an upright optical microscope Olympus BX51 (Japan). White light from the halogen lamp was focused onto the sample obliquely via an oil immersion dark field condenser (NA 1.2). Scattered light was collected using a 40× objective and then captured using a color CCD camera (DP70, Olympus).

**Immunofluorescence Analysis of Neuronal and Synaptic Proteins.** To determine the toxicity of different tau-R2 aggregates in cortical neurons, we performed immunocytochemical analysis of microtubule-associated protein 2 (MAP-2) and synaptophysin, which

are specific markers for neurons and synapses, respectively. After drug treatment, cells were fixed with 4% paraformaldehyde and then permeabilized with 0.2% Triton X-100 (Sigma). Samples were blocked for 1 h at room temperature and then incubated with a primary antibody diluted in a blocking solution overnight at 4 °C. MAP-2 (1:8000, chicken polyclonal, Abcam) and synaptophysin (1:200, rabbit monoclonal, Abcam) were probed. Cells were incubated with the primary antibody, followed by three times wash with PBS, and then incubated with either goat-antichichen-Alexa594 or goat-antirabbit-Alexa488 (both 1:200 dilution, Abcam) for 1 h at room temperature. After three times wash in PBS, coverslips were mounted on slides and cells imaged using a confocal microscope (Olympus FV1000).

**Time Lapse Photography of Mitochondrial Mobility.** Mitochondria were labeled by transfecting pDsRed2-mito plasmid (Clontech) into the cortical neurons at day 5 with lipofectamine 2000 (Invitrogen), according to the manufacturer's protocol. At day 8, neurons were treated with tau aggregates (7.5 $\mu$M tau-R2, 3.5 $\mu$M $Cu^{+}/Cu^{2+}$, 5 $\mu$M SelP-H, and 1.9 $\mu$M heparin, incubated at 37 °C for 6 h before added to the neurons) and then imaged 12 h later. A process 2−3 times longer than other processes stemming from the soma was considered to be an axon.[29] Mitochondria were identified as particles with strong labeling and clear edges confined in axons. Series of time-lapse images were captured every 5 s with a confocal microscope (Olympus FV1000) for a total of 2 min. Z-stacks for each time point were collapsed to maximum projections, and the time series were archived as avi files. ImageJ software, with a Multiple Kymograph plug-in, was used to analyze the avi files. Mitochondrial movements were determined from the kymographic images. Mitochondria were considered stationary if they did not move more than 2 $\mu$m during the entire recording period. Each series of images was recorded for at least three randomly selected Ds-Red-mito-labeled cells per culture and four independent cultures per condition.

## CONCLUSION

The thermodynamic properties of tau-R2 binding Cu ions in both oxidation states of $Cu^{+}$ and $Cu^{2+}$ were explored by spectroscopic and calorimetric methods. Tau-R2 was demonstrated to bind 0.44 $Cu^{2+}$ and 0.34 $Cu^{+}$ per monomer with dissociation constants of 1.1 nM and 0.2 pM, respectively. Copper ions binding to tau-R2 promoted tau-R2 aggregation, and the copper-associated tau-R2 aggregates stimulated intracellular ROS generation and death of N2A cell. Using the primarily cultured cortical neurons, tau-R2 aggregates, especially in the presence of copper ions, were demonstrated to decrease protein levels of MAP-2 and synaptophysin, the specific markers of neuron and synapse, and reduce mitochondrial density and mobility in the axon and as a consequence impair the growth and probably also the function of neurons. SelP-H, with higher affinity toward both $Cu^{2+}$ and $Cu^{+}$ than tau-R2, not only inhibited copper-mediated tau aggregation but also interfered with the ongoing aggregation and disaggregated the already formed aggregates. Interestingly, SelP-H significantly attenuated $Cu^{2+}/Cu^{+}$−tau-R2-induced intracellular ROS production and the impairments of synapse and mitochondria in neurons. SelP was found to be colocalized with A$\beta$ plaques and NFT in the postmortem tissues from individuals with the hallmark lesions of AD.[44] These studies suggest that in addition to its roles in Se transport and oxidant defense, SelP may play certain roles in regulating redox balance as well as metal homeostasis. In vivo studies using AD model mouse are underway to better understand the role of SelP in the brain and AD progress.

## ASSOCIATED CONTENT

### Supporting Information

Plot of $1/Y$ versus of $X$ to give the intrinsic binding constants and binding number of tau-R2 for $Cu^{+}$; effect of SelP-H on tau-R2 fibrillation in the absence of copper ions; typical dark field microscopy images of primary neurons upon treatment with copper ions; typical confocal images showing the levels and distributions of MAP-2 and synaptophysin in primary neurons upon treatment with copper ions; determination of intrinsic binding constants and binding number of tau-R2 for $Cu^{+}$ by competition with BCA for $Cu^{+}$; supplementary methods on "Estimation of $Cu^{+}$ binding constants". This material is available free of charge via the Internet at http://pubs.acs.org.

## AUTHOR INFORMATION

### Corresponding Authors

* E-mail: jzni@szu.edu.cn.
* E-mail: liuqiong@szu.edu.cn.

### Author Contributions

This manuscript was written through contributions of all authors. All authors have given approval to the final version of the manuscript.

### Notes

The authors declare no competing financial interest.

## ACKNOWLEDGMENTS

This work was financially supported by the National Natural Science Foundation of China (Nos. 31070731, 21271131, 21301120) and the Shenzhen Bureau of Science, Technology and Information (Nos. JCYJ20120817163755064, JCYJ20130408172946974). The TEM used in this work was supported by the Institute for Advanced Materials (IAM) with funding from the special Equipment Grant from the University Grants Committee of the Hong Kong Special Administrative Region, China (SEG_HKBU06).

## REFERENCES

(1) Mandelkow, E. M.; Mandelkow, E. *Cold Spring Harbor Perspect. Med.* **2012**, *2*, a006247.
(2) Arriagada, P. V.; Growdon, J. H.; Hedley-Whyte, E. T.; Hyman, B. T. *Neurology* **1992**, *42*, 631−9.
(3) Bancher, C.; Braak, H.; Fischer, P.; Jellinger, K. A. *Neurosci. Lett.* **1993**, *162*, 179−82.
(4) Polydoro, M.; Acker, C. M.; Duff, K.; Castillo, P. E.; Davies, P. *J. Neurosci.* **2009**, *29*, 10741−9.
(5) Small, S. A.; Duff, K. *Neuron* **2008**, *60*, 534−542.
(6) Bolognin, S.; Messori, L.; Drago, D.; Gabbiani, C.; Cendron, L.; Zatta, P. *Int. J. Biochem. Cell Biol.* **2011**, *43*, 877−85.
(7) Bramblett, G. T.; Goedert, M.; Jakes, R.; Merrick, S. E.; Trojanowski, J. Q.; Lee, V. M. *Neuron* **1993**, *10*, 1089−99.
(8) Sayre, L. M.; Perry, G.; Harris, P. L.; Liu, Y.; Schubert, K. A.; Smith, M. A. *J. Neurochem.* **2000**, *74*, 270−9.
(9) Shin, B. K.; Saxena, S. *J. Phys. Chem. B* **2011**, *115*, 15067−78.
(10) Ma, Q.; Li, Y.; Du, J.; Liu, H.; Kanazawa, K.; Nemoto, T.; Nakanishi, H.; Zhao, Y. *Peptides* **2006**, *27*, 841−9.
(11) Bellinger, F. P.; Raman, A. V.; Rueli, R. H.; Bellinger, M. T.; Dewing, A. S.; Seale, L. A.; Andres, M. A.; Uyehara-Lock, J. H.; White, L. R.; Ross, G. W.; Berry, M. J. *J. Parkinson Dis.* **2012**, *2*, 115−26.
(12) Bellinger, F. P.; He, Q. P.; Bellinger, M. T.; Lin, Y.; Raman, A. V.; White, L. R.; Berry, M. J. *J. Alzheimers Dis.* **2008**, *15*, 465−72.
(13) Du, X.; Li, H.; Wang, Z.; Qiu, S.; Liu, Q.; Ni, J. *Metallomics* **2013**, *5*, 861−70.
(14) Du, X.; Wang, Z.; Zheng, Y.; Li, H.; Ni, J.; Liu, Q. *Inorg. Chem.* **2014**, *53*, 1672−8.

(15) Wille, H.; Drewes, G.; Biernat, J.; Mandelkow, E. M.; Mandelkow, E. *J. Cell. Biol.* **1992**, *118*, 573−584.
(16) Berriman, J.; Serpell, L. C.; Oberg, K. A.; Fink, A. L.; Goedert, M.; Crowther, R. A. *Proc. Natl. Acad. Sci. U.S.A.* **2003**, *100*, 9034−8.
(17) Tomoo, K.; Yao, T. M.; Minoura, K.; Hiraoka, S.; Sumida, M.; Taniguchi, T.; Ishida, T. *J. Biochem.* **2005**, *138*, 413−23.
(18) von Bergen, M.; Friedhoff, P.; Biernat, J.; Heberle, J.; Mandelkow, E. M.; Mandelkow, E. *Proc. Natl. Acad. Sci. U.S.A.* **2000**, *97*, 5129−5134.
(19) Soragni, A.; Zambelli, B.; Mukrasch, M. D.; Biernat, J.; Jeganathan, S.; Griesinger, C.; Ciurli, S.; Mandelkow, E.; Zweckstetter, M. *Biochemistry* **2008**, *47*, 10841−10851.
(20) Ma, Q. F.; Li, Y. M.; Du, J. T.; Kanazawa, K.; Nemoto, T.; Nakanishi, H.; Zhao, Y. F. *Biopolymers* **2005**, *79*, 74−85.
(21) Ma, Q. F.; Li, Y. M.; Du, J. T.; Liu, H.; Kanazawa, K.; Nemoto, T.; Nakanishi, H.; Zhao, Y. F. *Peptides* **2006**, *27*, 841−849.
(22) Xiao, Z.; Donnelly, P. S.; Zimmermann, M.; Wedd, A. G. *Inorg. Chem.* **2008**, *47*, 4338−47.
(23) Grossoehme, N. E.; Spuches, A. M.; Wilcox, D. E. *J. Biol. Inorg. Chem.* **2010**, *15*, 1183−91.
(24) Du, X.; Li, H.; Wang, X.; Liu, Q.; Ni, J.; Sun, H. *Chem. Commun.* **2013**, *49*, 9134−6.
(25) Sacco, C.; Skowronsky, R. A.; Gade, S.; Kenney, J. M.; Spuches, A. M. *J. Biol. Inorg. Chem.* **2012**, *17*, 531−41.
(26) Shearer, J.; Szalai, V. A. *J. Am. Chem. Soc.* **2008**, *130*, 17826−35.
(27) Flach, K.; Hilbrich, I.; Schiffmann, A.; Gartner, U.; Kruger, M.; Leonhardt, M.; Waschipky, H.; Wick, L.; Arendt, T.; Holzer, M. *J. Biol. Chem.* **2012**, *287*, 43223−33.
(28) Hondal, R. J.; Ma, S.; Caprioli, R. M.; Hill, K. E.; Burk, R. F. *J. Biol. Chem.* **2001**, *276*, 15823−31.
(29) Du, H.; Guo, L.; Yan, S.; Sosunov, A. A.; McKhann, G. M.; Yan, S. S. *Proc. Natl. Acad. Sci. U.S.A.* **2010**, *107*, 18670−5.
(30) Calkins, M. J.; Reddy, P. H. *Biochim. Biophys. Acta* **2011**, *1812*, 507−13.
(31) Ebneth, A.; Godemann, R.; Stamer, K.; Illenberger, S.; Trinczek, B.; Mandelkow, E. *J. Cell. Biol.* **1998**, *143*, 777−94.
(32) Kopeikina, K. J.; Carlson, G. A.; Pitstick, R.; Ludvigson, A. E.; Peters, A.; Luebke, J. I.; Koffie, R. M.; Frosch, M. P.; Hyman, B. T.; Spires-Jones, T. L. *Am. J. Pathol.* **2011**, *179*, 2071−82.
(33) Amadoro, G.; Corsetti, V.; Stringaro, A.; Colone, M.; D'Aguanno, S.; Meli, G.; Ciotti, M.; Sancesario, G.; Cattaneo, A.; Bussani, R.; Mercanti, D.; Calissano, P. *J. Alzheimers Dis.* **2010**, *21*, 445−470.
(34) Liu, L.; Drouet, V.; Wu, J. W.; Witter, M. P.; Small, S. A.; Clelland, C.; Duff, K. *Plos One* 2012, *7*.
(35) Frost, B.; Jacks, R. L.; Diamond, M. I. *J. Biol. Chem.* **2009**, *284*, 12845−12852.
(36) Clavaguera, F.; Bolmont, T.; Crowther, R. A.; Abramowski, D.; Frank, S.; Probst, A.; Fraser, G.; Stalder, A. K.; Beibel, M.; Staufenbiel, M.; Jucker, M.; Goedert, M.; Tolnay, M. *Nat. Cell Biol.* **2009**, *11*, 909−U325.
(37) de Calignon, A.; Polydoro, M.; Suarez-Calvet, M.; William, C.; Adamowicz, D. H.; Kopeikina, K. J.; Pitstick, R.; Sahara, N.; Ashe, K. H.; Carlson, G. A.; Spires-Jones, T. L.; Hyman, B. T. *Neuron* **2012**, *76*, 461−461.
(38) Goedert, M.; Spillantini, M. G. *Science* **2006**, *314*, 777−81.
(39) Karch, C. M.; Jeng, A. T.; Goate, A. M. *J. Bio;. Chem.* **2012**, *287*, 42751−42762.
(40) Pooler, A. M.; Phillips, E. C.; Lau, D. H. W.; Noble, W.; Hanger, D. P. *EMBO Rep.* **2013**, *14*, 389−394.
(41) Saman, S.; Kim, W.; Raya, M.; Visnick, Y.; Miro, S.; Saman, S.; Jackson, B.; McKee, A. C.; Alvarez, V. E.; Lee, N. C. Y.; Hall, G. F. *J. Biol. Chem.* **2012**, *287*, 3842−3849.
(42) Rae, T. D.; Schmidt, P. J.; Pufahl, R. A.; Culotta, V. C.; O'Halloran, T. V. *Science* **1999**, *284*, 805−808.
(43) Herd, S. M.; Camakaris, J.; Christofferson, R.; Wookey, P.; Danks, D. M. *Biochem. J.* **1987**, *247*, 341−7.
(44) Bellinger, F. P.; He, Q. P.; Bellinger, M. T.; Lin, Y.; Raman, A. V.; White, L. R.; Berry, M. J. *J. Alzheimers Dis.* **2008**, *15*, 465−72.
(45) Hoffmann, P. R.; Hoge, S. C.; Li, P. A.; Hoffmann, F. W.; Hashimoto, A. C.; Berry, M. J. *Nucleic Acids Res.* **2007**, *35*, 3963−73.
(46) Burk, R. F.; Hill, K. E. *Annu. Rev. Nutr.* **2005**, *25*, 215−35.

## NOTE ADDED AFTER ASAP PUBLICATION

This paper was published on the Web on October 7, 2014, with incorrect information for references 23 and 25. The corrected version was reposted on October 9, 2014.